Elastic magnetic form factors of exotic nuclei

Tiekuang Dong,[1,3,*] Zhongzhou Ren,[1,2,3] and Yanqing Guo[1,3]

[1]*Department of Physics, Nanjing University, Nanjing 210008, People's Republic of China*

[2]*Center of Theoretical Nuclear Physics, National Laboratory of Heavy-Ion Accelerator, Lanzhou 730000, People's Republic of China*

[3]*Joint Center for Particle, Nuclear Physics and Cosmology, Nanjing 210008, People's Republic of China*

(Received 19 May 2007; revised manuscript received 10 September 2007; published 14 November 2007)

How to identify the orbital of the valence nucleon(s) of exotic nuclei is an important problem. The elastic magnetic electron scattering is an excellent probe to determine the valence structure of odd-*A* nuclei. The relativistic mean-field theory has been successfully applied to systematic studies of the elastic charge electron scattering from even-even exotic nuclei. The extension of this method to investigate the elastic magnetic electron scattering from odd-*A* exotic nuclei is a natural generalization. The experimental form factors of ^{17}O and ^{41}Ca are reproduced very well with the help of the spectroscopic factors which are introduced into the relativistic treatment of the magnetic electron scattering for the first time. The emphases are put on the magnetic form factors of ^{15,17,19}C, ^{23}O, ^{17}F, and ^{49,59}Ca calculated in the relativistic impulse approximation. Great differences have been found in the form factors of the same nucleus with different configurations. Therefore, the elastic magnetic electron scattering can be used to determine the orbital of the last nucleon of odd-*A* exotic nuclei. Our results can provide references for the electron scattering from exotic nuclei in the near future.

DOI: 10.1103/PhysRevC.76.054602 PACS number(s): 27.20.+n, 24.10.−i, 25.30.Bf

I. INTRODUCTION

In the past 20 years, the nuclear structure of halo nuclei have attracted much attention [1–3]. Very recently, Wang *et al.* [4] have studied the observable effects of the extended charge densities on the form factors of the elastic charge electron scattering from even-even exotic nuclei by comparing with those from stable ones. A halo nucleus can be viewed as a normal core plus a low density halo. The formation of a halo is directly related to the orbital of the last nucleon(s). As for odd-*A* exotic nuclei, the orbital of the last nucleon is mainly deduced from the ground-state spin-parity and the spectroscopic factors up to now. However, the spin-parity of an exotic nucleus is not always available. When the spin-parity is absent, there may exist debate about the configuration of the exotic nucleus. For example, the configuration of ^{23}O arose a hot debate very recently [5–10]. A similar situation has ever occurred for ^{19}C [11]. The nuclear density distribution is another important property of nuclei. It is an important input of some reaction models such as the most-used Glauber model. As for two-body halo nuclei (i.e., one-nucleon halo nuclei) the density can be viewed as the sum of the normal core density and the halo density which is determined by the orbital of the last nucleon. Therefore, a sensitive probe that can determine accurately both the orbital and the density of the halo nucleon is necessary. Elastic magnetic electron scattering provides us such a probe [12–14]. Elastic magnetic electron scattering has been extensively used to study the valence structure of the nuclei near the stability valley. The magnetic form factor is determined by the orbital of the last nucleon. So from the elastic magnetic form factor one can determine directly the orbital of the last nucleon. Furthermore, electron is a charged lepton, which can only participate in electromagnetic interaction. It is expected that in the process of electron scattering the wave function of the loosely bound halo nucleon can hardly be perturbed. Therefore, magnetic electron scattering will be a powerful tool in studying the valence structure of exotic nuclei. In recent years, an electron scattering ring is under construction at RIKEN [2,15,16] in Japan. Similar facilities are also under construction or planned to be constructed [17,18]. It is expected that the data of electron scattering from exotic nuclei will be available soon. Therefore, it is time to study the magnetic electron scattering from exotic nuclei, providing references for future experiments. In fact, Bertulani [19] and Karataglidis *et al.* [20] have performed theoretical studies on electron scattering from exotic nuclei very recently.

In order to calculate the magnetic form factor we need a reliable model to provide the single-particle wave function. In the literature, the magnetic form factors of electron scattering from stable nuclei were often calculated using the single-particle wave functions of the Woods-Saxon model. Although this method has given reliable results for odd-*A* nuclei near the stability line, the not well-known dependence of the nuclear potential on proton and neutron numbers of exotic nuclei [2] make it invalid at present. Moreover, the wave function of the last nucleon is also determined by its binding (or separation) energy. Unfortunately, the one-nucleon separation energies of exotic nuclei are very difficult to measure. For instance, in the 1995 mass table by Audi *et al.* [21] the one-neutron separation energy S_n of ^{19}C is 160(110) keV, and in the 2003 mass table [22] this value is replaced by 580(90) keV which is close to the value 530(130) keV deduced by Nakamura *et al.* [23]. Therefore, a self-consistent model is required in calculating the single-particle wave function of the last nucleon. As a simple model of the quantum hadronic dynamics (QHD), the relativistic mean-field (RMF) theory is a good choice. This model has been successful in studying the halo structure [4,24]. The QHD models have also achieved success

*tkdong99@gmail.com

in investigating the magnetic properties of odd-A nuclei. Serot [25] and Kim [26] have calculated the elastic magnetic form factors in the relativistic impulse approximation. An obvious advantage of the QHD is that it provides a consistent framework to examine various corrections such as the effects of the backflow [27–29] and the meson exchange currents (MEC) [30]. As the first step to investigate the magnetic form factors of exotic nuclei in the QHD framework, we will neglect these corrections since the purpose of this paper is to suggest a method of identifying the configurations of exotic nuclei rather than making comparisons with existing data. More detailed calculations will be performed in the next works. In this paper, we will calculate the magnetic form factors of ^{23}O, ^{17}F, ^{49,59}Ca, and ^{15,17,19}C in the plane wave Born approximation (PWBA) for simplicity.

II. THEORY

In the RMF theory [31–33], the single-particle wave function of the valence nucleon reads (following the notation of Ref. [34])

$$\psi_{n\kappa m} = \begin{bmatrix} i[G(r)/r]\Phi_{\kappa m}(\hat{r}) \\ -[F(r)/r]\Phi_{-\kappa m}(\hat{r}) \end{bmatrix} = \begin{bmatrix} i|n\kappa m\rangle \\ -\overline{|n\kappa m\rangle} \end{bmatrix} = \begin{bmatrix} i\left|\mathrm{nl}\frac{1}{2}jm\right\rangle \\ -\left|\mathrm{nl}'\frac{1}{2}jm\right\rangle \end{bmatrix}. \quad (1)$$

With above relative phase factor the upper and lower components $G(r)$ and $F(r)$ are real functions. The angular quantum number κ uniquely determines the orbital and the total angular momentum quantum numbers l, l', and j,

$$j = |\kappa| - \frac{1}{2}, \quad \begin{cases} l = \kappa, & l' = l-1, \quad (\kappa > 0) \\ l = -(\kappa+1), & l' = l+1, \quad (\kappa < 0). \end{cases} \quad (2)$$

In Eq. (1) $\Phi_{\kappa m}$ is the spinor spherical harmonics.

In the quantum hadronic dynamics (QHD) the internal structure of the single nucleon comes mainly from the charged mesons. In the low and medium momentum transfer region (say $q \leqslant 5$ fm^{-1}) it is reliable to assume that the free single nucleon charge and magnetic form factors have the same q dependence:

$$F_{1,2}(q^2) = f_{\mathrm{sn}}(q^2)F_{1,2}(0), \quad (3)$$

where q is the momentum transfer carried by the virtual photon. Then the S-matrix of electron scattering from a single nucleon is equivalent to that from the effective current operator [25,26,35]

$$\hat{J}_\mu = i\bar{\psi}Q\gamma_\mu\psi + (1/2M_n)\partial/\partial x_\nu(\bar{\psi}\lambda'\sigma_{\mu\nu}\psi). \quad (4)$$

In this equation Q (M_n) is the charge (mass) of the nucleon and λ' is the anomalous magnetic moment [36],

$$Q = \frac{1}{2}(1+\tau_3), \quad \lambda' = \frac{\lambda'_p}{2}(1+\tau_3) + \frac{\lambda'_n}{2}(1-\tau_3), \quad (5)$$

with $\lambda'_p = 1.793$, $\lambda'_n = -1.913$.

The magnetic form factor can be expressed in terms of the reduced matrix elements of the magnetic multipole operators of the effective current operator,

$$F^2_{\mathrm{ML}}(q) = \frac{4\pi}{2J_i+1}|\langle J_f\|\hat{T}^{\mathrm{mag}}_L(q)\|J_i\rangle|^2. \quad (6)$$

The multipole operator is given by [12–14]

$$\hat{T}^{\mathrm{mag}}_{\mathrm{LM}}(q) = \int j_L(qr)\mathbf{Y}^{\mathbf{M}}_{\mathbf{LL}}(\hat{r})\cdot\hat{\mathbf{J}}(\mathbf{r})d^3\mathbf{r}, \quad (7)$$

where $\mathbf{Y}^{\mathbf{M}}_{\mathbf{LL}}(\hat{\mathbf{r}})$ is the vector spherical harmonics [37]. With the effective current operator and the four-component Dirac wave function the multipole operator $\hat{T}^{\mathrm{mag}}_{\mathrm{LM}}$ can be written in a block matrix form [25,26,35]:

$$\hat{T}^{\mathrm{mag}}_{\mathrm{LM}}(\mathbf{r}) = \begin{bmatrix} iq(\lambda'/2M_n)\Sigma'^M_L(\mathbf{r}) & Q\Sigma^M_L(\mathbf{r}) \\ Q\Sigma^M_L(\mathbf{r}) & -iq(\lambda'/2M_n)\Sigma'^M_L(\mathbf{r}) \end{bmatrix}, \quad (8)$$

where

$$\Sigma^M_L(\mathbf{r}) \equiv \mathbf{M}^{\mathbf{M}}_{\mathbf{LL}}(\mathbf{r})\cdot\sigma,$$
$$\Sigma'^M_L(\mathbf{r}) \equiv -i(\nabla\times\mathbf{M}^{\mathbf{M}}_{\mathbf{LL}}(\mathbf{r}))\cdot\sigma/q,$$
$$\mathbf{M}^{\mathbf{M}}_{\mathbf{LL}}(\mathbf{r}) \equiv j_L(qr)\mathbf{Y}^{\mathbf{M}}_{\mathbf{LL}}(\hat{\mathbf{r}}).$$

In the independent single-particle shell model only the last nucleon contributes to the magnetic form factor

$$\begin{aligned} F^2_M(q) &= \frac{4\pi f^2_{\mathrm{sn}}(q)f^2_{\mathrm{c.m.}}(q)}{2J_i+1}\sum_{L=1}^{\mathrm{odd}}|\langle J_f\|\hat{T}_L{}^{\mathrm{mag}}\|J_i\rangle|^2 \\ &= \frac{4\pi f^2_{\mathrm{sn}}(q)f^2_{\mathrm{c.m.}}(q)}{2J_i+1}\sum_{L=1}^{\mathrm{odd}}|2\overline{\langle n\kappa\|}Q\Sigma_L\|n\kappa\rangle - (q/2M_n) \\ &\quad\times(\langle n\kappa\|\lambda'\Sigma'_L\|n\kappa\rangle - \overline{\langle n\kappa\|}\lambda'\Sigma'_L\overline{\|n\kappa\rangle})|^2, \end{aligned} \quad (9)$$

where the single-nucleon factor and the center-of-mass factor are given by $f_{\mathrm{sn}}(q) = [1+(q/855\,\mathrm{MeV})^2]^{-2}$ and $f_{\mathrm{c.m.}}(q) = \exp(q^2b^2/4A)$, respectively. In this paper we choose the oscillator parameter $b = A^{1/6}$ fm^{-1}.

In calculating the single-particle reduced matrix elements the formulas given by Edmonds [37] and Willey [38] are used. With the method of partial integration the reduced matrix elements can be written explicitly as follows:

$$\begin{aligned} &\langle n\kappa\|\Sigma'_L\|n\kappa\rangle \\ &= \frac{(-1)^{l+1}}{q}\left(\frac{6}{4\pi}\right)^{1/2}(2l+1)(2j+1) \\ &\quad\times\left[\begin{Bmatrix} l & l & L+1 \\ \frac{1}{2} & \frac{1}{2} & 1 \\ j & j & L \end{Bmatrix}\begin{pmatrix} l & L+1 & l \\ 0 & 0 & 0 \end{pmatrix}(L(2L+3))^{1/2}\right. \\ &\quad\times\int dr\,r^2 j_L(qr)\left(\frac{d}{dr}+\frac{L+2}{r}\right)g^2(r) \\ &\quad+\begin{Bmatrix} l & l & L-1 \\ \frac{1}{2} & \frac{1}{2} & 1 \\ j & j & L \end{Bmatrix}\begin{pmatrix} l & L-1 & l \\ 0 & 0 & 0 \end{pmatrix}((L+1)(2L-1))^{1/2} \\ &\quad\times\left.\int dr\,r^2 j_L(qr)\left(\frac{d}{dr}-\frac{L-1}{r}\right)g^2(r)\right], \end{aligned} \quad (10)$$

and

$$\overline{\langle n\kappa\|\Sigma_L\|n\kappa\rangle} = (-1)^{l'}\left(\frac{6}{4\pi}\right)^{1/2}(2L+1)(2j+1)((2l+1)(2l'+1))^{1/2} \times \begin{Bmatrix} l' & l & L \\ \frac{1}{2} & \frac{1}{2} & 1 \\ j & j & L \end{Bmatrix} \times \begin{pmatrix} l' & L & l \\ 0 & 0 & 0 \end{pmatrix} \int dr\, r^2 j_L(qr) g(r) f(r), \tag{11}$$

where we have defined $g(r) = G(r)/r$, $f(r) = F(r)/r$. Through replacing $g(r)$ and l by $f(r)$ and l' of Eq. (10), respectively, one can obtain the matrix element $\overline{\langle n\kappa\|\Sigma'_L\|n\kappa\rangle}$.

III. NUMERICAL RESULTS

With the formalism described above we write the fortran code. At first, it is necessary to investigate the validity and precision of this code. With this purpose, we calculate the elastic magnetic form factors of ^{17}O and ^{41}Ca where the last neutron has a stretched configuration ($j = l + \frac{1}{2}$) and is bound by the doubly closed core. For these nuclei, the interpretation of magnetic form factors is very simple. That is why we choose these two nuclei to test the validity of this code. The nonlinear RMF calculations are performed with the force parameters NL-SH [32] and TM1/TM2 [33]. Many calculations showed that these parameters can reproduce the ground-state properties of both stable and unstable nuclei. The theoretical results of ^{17}O and ^{41}Ca calculated using the relativistic formulas agree with the experimental data considerably. The detailed results are shown in Fig. 1. It is shown that the single-particle form factors deviate slightly from the experimental data in low and medium q region, and that the single-particle form factors fall more steeply than experimental data. These deviations are attributed to the many-body effects such as backflow and meson exchange currents in the relativistic field theory. Historically, the discrepancies between the experimental and theoretical results were often treated by introducing the spectroscopic factors α'_Ls which were fitted along with the parameters of the Woods-Saxon model. In this paper we will also make the least-square fits to the form factors using the formula

$$F_M^2 = \sum_{L=1}^{\text{odd}} \alpha_L^2 F_{\text{ML}}^2(q) f_{\text{sn}}^2(q) f_{\text{c.m.}}^2(q). \tag{12}$$

For the first time, the spectroscopic factors are introduced into the relativistic treatment of the magnetic form factors. However, it can not be generalized simply from the non-relativistic models to the relativistic ones. There is a question must be answered beforehand: do these corrections depend strongly on the momentum transfer in the relativistic field-theories? The answer is no. Ichii *et al*. [28] have shown that the effect of vacuum fluctuation (or backflow) is moderate and changes slowly with the momentum transfer. Blunden and Kim [30] have calculated the contributions of the one-pion exchange currents and found a fairly uniform enhancement of the magnetic form factors up to a rather high momentum transfer $q = 4$ fm^{-1}. Therefore, it is reasonable to believe that these effects can be incorporated into the spectroscopic factors sufficiently. In contrast to the nonrelativistic treatment where the parameters of the single-particle potential are fitted simultaneously with the spectroscopic factors, we assume the validity of the RMF theory in predicting the wave function of the last nucleon beforehand. The purpose is twofold: one is to see to what extent the discrepancy can be eliminated in both low and high q regions; the other is to compare these spectroscopic factors with those obtained from the Woods-Saxon model. Because of the lack of experimental data in the very low q region where $M1$ dominates the electron scattering, the factor α_1 is fixed to the ratio of the experimental magnetic moment to the single-particle value: $\alpha_1 = \mu_{\text{exp}}/\mu_{\text{sp}}$. The experimental and single-particle magnetic moments, rms radii of the valence neutron, and spectroscopic factors are listed in Table I. In this table the experimental magnetic moments of these two nuclei are both taken from the table compiled by Raghavan [39].

For ^{17}O, the rms radii of the $1d_{5/2}$ orbital calculated from the RMF theory with parameters NL-SH and TM2 are 3.397 fm and 3.458 fm, respectively. These results agree with the values of Refs. [40–42]. The valence rms radius of ^{17}O deduced from the best fit of the overall spectroscopic factors $\alpha'_L s$ to the magnetic electron scattering data taken from Ref. [43] is 3.35 ± 0.03 fm [41], which is very close to the value 3.36 fm of Ref. [40]. The spectroscopic factors of $M5$ from NL-SH and TM2 are 0.92 and 0.94, respectively. These values are similar to the value 0.96±0.11 deduced from elastic electron scattering form factors in the high-q region [40]. As for ^{41}Ca, the rms radius of the $1f_{7/2}$ orbital obtained from sub-Coulomb transfer reactions are 4.00 ± 0.06 fm [44] and 3.89 ± 0.12 fm [45]. These values are similar to the results deduced from elastic electron scattering data 3.99 ± 0.06 fm [46] and 3.99 ± 0.05 fm [47]. The RMF results 4.01 and 4.12 fm agree well with the value 4.02 fm from the nonrelativistic mean-field theory [48]. The spectroscopic factors of $M7$ (see Table I) are also in agreement with the value 0.83 ± 0.05 obtained in Ref. [46]. The agreement of the

TABLE I. Valence rms radii (in fm), magnetic moments (in μ_N), and spectroscopic factors of ^{17}O and ^{41}Ca.

Nucleus	Configuration	Force	rms	μ_{exp}	μ_{sp}	α_1	α_3	α_5	α_7
^{17}O	$1d_{5/2}$	NLSH	3.397	−1.894	−1.913	0.99	0.46	0.92	
^{17}O		TM2	3.458			0.99	0.40	0.94	
^{41}Ca	$1f_{7/2}$	NLSH	4.014	−1.595	−1.913	0.83	0.70	0.56	0.87
^{41}Ca		TM2	4.118			0.83	0.71	0.52	0.89

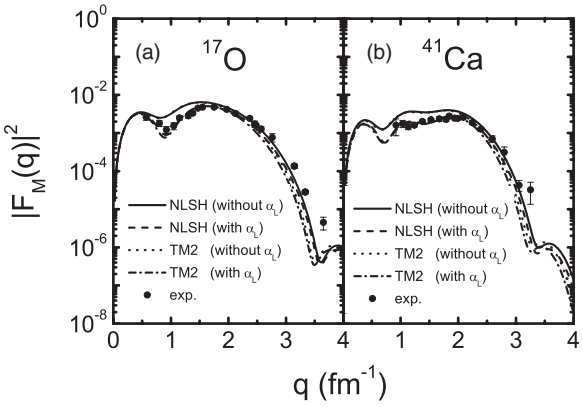

FIG. 1. The magnetic form factors of ^{17}O and ^{41}Ca. The single-particle form factors are labeled by "without α_L", the results including the spectroscopic factors are labeled by "with α_L". The experimental form factors of ^{17}O and ^{41}Ca are taken from Refs. [40,43] and [46,47], respectively.

rms radii and spectroscopic factors in the RMF theory with the experimental data and other theoretical ones implies the validity of the RMF theory in reproducing the magnetic form factor.

The theoretical form factors with and without the spectroscopic factors are shown in Fig. 1. In this figure, the experimental form factors of ^{17}O and ^{41}Ca are taken from Refs. [40,43] and [46,47], respectively. One can see that the theoretical form factors of ^{17}O and ^{41}Ca with the spectroscopic factors agree very well with the experimental data in low and medium q region, but in high-q region the theoretical form factors still fall more deeply than the experimental data. It means that the discrepancy in high-q region can not be eliminated only by introducing the spectroscopic factors. The reason is that in the high-q region the large momentum virtual photon may excite more degrees of freedom, such as the Δ-isobar, and even quark structure of hadrons, and more than one particles may share the momentum transfer carried by the virtual photon.

With the assumption that the RMF theory is valid in predicting the single-particle wave function of the last nucleon of exotic nuclei, we calculate the elastic form factors of ^{23}O using the formulas given in Sec. II. The single-particle wave function of the last neutron is obtained from the nonlinear RMF theory with NL-SH and TM2 parameters. The calculations are performed for two cases: (a) the last neutron occupies the $1d_{5/2}$ orbital, and (b) the last neutron occupies the $2s_{1/2}$ orbital. For case (a) the configuration of ^{23}O is $(1d_{5/2})^5(2s_{1/2})^2$, and the configuration for case (b) is $(1d_{5/2})^6(2s_{1/2})^1$. The results are listed in Table II. In this table $(B/A)_{\rm cal.}$ is the theoretical average binding energy (in MeV), R_c, R_n, R_m are rms radii (in fm) of the charge, neutron, and matter densities, R_v is the rms radius of the last neutron (in fm), and ϵ's are single-particle energy levels (in MeV). The experimental average binding energy is taken from the 2003 Audi Table [22]. It is clear that the results from NL-SH and TM2 are close to each other. It means that the RMF theory is stable in predicting the properties of exotic nuclei. So we will only show the results from NL-SH in the next.

TABLE II. The ground-state properties of ^{23}O calculated using NL-SH and TM2 parameters. The experimental average binding energy is 7.164 MeV [22].

	$1d_{5/2}$ (NLSH)	$2s_{1/2}$ (NLSH)	$1d_{5/2}$ (TM2)	$2s_{1/2}$ (TM2)
$(B/A)_{\rm cal.}$	7.097	7.248	7.155	7.325
R_c(fm)	2.723	2.712	2.776	2.763
R_n(fm)	3.224	3.128	3.308	3.205
R_m(fm)	3.022	2.951	3.096	3.021
R_v(fm)	3.472	4.453	3.549	4.649
$-\epsilon(1s_{1/2})$ (p)	48.47	49.20	48.97	49.74
$-\epsilon(1p_{3/2})$ (p)	29.34	30.46	29.78	31.01
$-\epsilon(1p_{1/2})$ (p)	22.63	24.09	22.42	24.02
$-\epsilon(1s_{1/2})$ (n)	43.22	43.70	43.41	43.82
$-\epsilon(1p_{3/2})$ (n)	24.13	24.41	24.15	24.46
$-\epsilon(1p_{1/2})$ (n)	17.57	18.27	16.96	17.75
$-\epsilon(1d_{5/2})$ (n)	7.23	7.31	7.35	7.46
$-\epsilon(2s_{1/2})$ (n)	3.82	3.73	3.60	3.43

When the last neutron occupies the $1d_{5/2}$ orbital (case (a)) the rms radius of the last neutron is much smaller than that when the last neutron occupies the $2s_{1/2}$ orbital [case (b)]. However, the rms radius of the total neutron distribution in case (a) is slightly larger than that in case (b). It is because there are two neutrons in the $2s_{1/2}$ orbital for case (a). In this case, the ground-state spin-parity is determined by the neutron in the d orbital and the neutrons in the s orbital participate in the nuclear reaction [5]. Whereas, in case (b) the ground-state spin-parity and the nuclear reaction are both determined by the same neutron in the s orbital. The density distribution calculated with NL-SH is shown in Fig. 2. In this figure, the lower part corresponds to case (a) and the upper part to case (b). One can see that the charge, neutron, and matter distributions are similar for these two cases. So it is difficult to determine the orbital of the last neutron from the rms radius which can be deduced from the total interaction cross section σ_I. Other experiments are

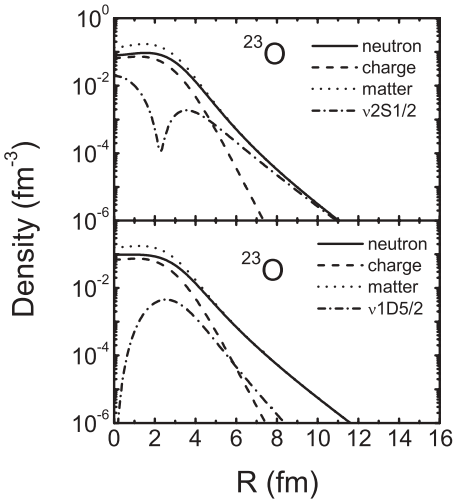

FIG. 2. The density distribution of ^{23}O when the last neutron occupies the $1d_{5/2}$ orbital (labeled by ν1D5/2) and the $2s_{1/2}$ orbital (labeled by ν2S1/2) from NL-SH.

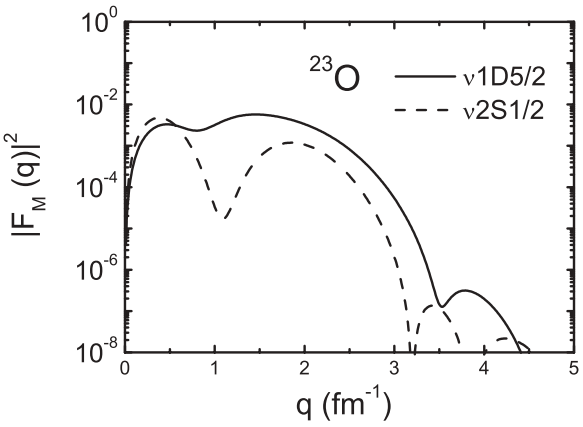

FIG. 3. The calculated form factors of ^{23}O when the last neutron occupies the $1d_{5/2}$ orbital (labeled by ν1D5/2) and the $2s_{1/2}$ orbital (labeled by ν2S1/2) from NL-SH.

needed. One-neutron knockout reaction [8], Coulomb breakup reaction [9], and one-neutron transfer reaction [10] have been performed and conclude that ^{23}O is a one-neutron halo nucleus with the last neutron occupying the $2s_{1/2}$ orbital. But there exist large deviations between the experimental data and the theoretical predictions, which are partly due to the complexity of the nuclear reaction mechanism which are not well-known up to now. Therefore, it is necessary to search for a simple and well-known probe to investigate the refine information of halo nuclei. The elastic magnetic electron scattering is a good choice.

The magnetic form factors from NL-SH are shown in Fig. 3. It is clear that there are great differences between the form factors of different configurations. Generally speaking, the form factor for the $2s_{1/2}$ orbital is smaller than that for the $1d_{5/2}$ orbital. Especially, near the first minimum the difference is up to a factor of about 100. When the elastic magnetic electron scattering form factors are obtained in the future, it will be very easy to determine the orbital of the last neutron from the shape of the measured form factor. After further analyses one can deduce the wave function and density distribution of the last neutron.

We are also interested in C isotopes ^{15,17,19}C. In this isotopic chain, ^{15}C and ^{19}C are both one-neutron halo nuclei but ^{17}C is not a halo nucleus. It means that this isotopic chain can provide much more knowledge about nuclear structure of exotic nuclei. We perform the RMF calculations of ^{15,17,19}C also for two cases: (a) the last neutron occupies the $1d_{5/2}$ orbital, and (b) the last neutron occupies the $2s_{1/2}$ orbital. For ^{15}C, case (a) corresponds to the configuration $(1d_{5/2})^1(2s_{1/2})^0$, and case (b) to $(1d_{5/2})^0(2s_{1/2})^1$ in the *sd* shell; for ^{17}C, case (a) corresponds to $(1d_{5/2})^1(2s_{1/2})^2$, case (b) to $(1d_{5/2})^2(2s_{1/2})^1$; for ^{19}C, case (a) corresponds to $(1d_{5/2})^3(2s_{1/2})^2$, case (b) to $(1d_{5/2})^4(2s_{1/2})^1$. The numerical results from NL-SH are listed in Table III. One can see that in the RMF theory the energy levels of the $1d_{5/2}$ and $2s_{1/2}$ orbitals in ^{15,17}C are very close. This agrees with the shell model prediction [11]. For example, the difference between $1d_{5/2}$ level and $2s_{1/2}$ level in ^{17}C is almost zero in the RMF theory with NL-SH parameters (see Table III). When the last neutron in ^{15}C occupies the $2s_{1/2}$ orbital [case (b)], the rms radii of the last neutron and the total neutron density increase sharply as compared with those when the last neutron occupies the $1d_{5/2}$ orbital [case (a)], though the level energies of these orbitals and the total binding energies are similar. The reason is that the rms radius of a level is determined by the detailed behavior of the wave function. A more node in the $2s_{1/2}$ orbital allows the extension of the wave function to larger coordinate compared with that of the $1d_{5/2}$ orbital. It is well known that the single-particle energy increases with both the number of node and the angular momentum. The halo nucleon favors the orbital with more nodes and low angular momentum which combine to make the nucleon have both larger binding energy and larger radius [24]. The rms radius of the total neutron density of ^{15}C in case (b) is much larger than that in case (a). The reason is that there is only one neutron in the *sd* shell. So it is possible to determine the orbital of the last neutron by comparing the radius of ^{15}C with neighboring nuclei such as ^{14}C, ^{15}N. As for ^{17}C and ^{19}C the situation is different. The total neutron radii of ^{17}C and

TABLE III. The ground-state properties of C isotopes calculated using NL-SH parameters. The experimental average binding energies of ^{15,17,19}C are 7.10017, 6.5576, and 6.118 MeV [22], respectively.

	^{15}C($1d_{5/2}$)	^{15}C($2s_{1/2}$)	^{17}C($1d_{5/2}$)	^{17}C($2s_{1/2}$)	^{19}C($1d_{5/2}$)	^{19}C($2s_{1/2}$)
$(B/A)_{\text{cal.}}$(MeV)	7.147	7.155	6.437	6.440	5.964	5.980
R_c(fm)	2.518	2.520	2.536	2.534	2.553	2.552
R_n(fm)	2.737	3.077	3.346	3.150	3.347	3.212
R_m(fm)	2.602	2.821	3.047	2.908	3.085	2.985
R_v(fm)	3.845	5.666	3.823	5.160	3.758	4.869
$-\epsilon(1s_{1/2})$ (p)	43.208	42.299	44.670	45.521	47.872	48.598
$-\epsilon(1p_{3/2})$ (p)	20.852	19.582	22.109	23.316	25.772	26.914
$-\epsilon(1p_{1/2})$ (p)	12.818	11.300	13.869	15.353	17.833	19.318
$-\epsilon(1s_{1/2})$ (n)	40.376	40.050	40.205	40.518	40.643	40.931
$-\epsilon(1p_{3/2})$ (n)	18.128	17.857	18.402	18.654	19.168	19.391
$-\epsilon(1p_{1/2})$ (n)	10.478	9.905	10.552	11.115	11.691	12.266
$-\epsilon(1d_{5/2})$ (n)	1.058	0.897	1.698	1.837	2.613	2.728
$-\epsilon(2s_{1/2})$ (n)	1.065	1.060	1.707	1.696	2.362	2.341

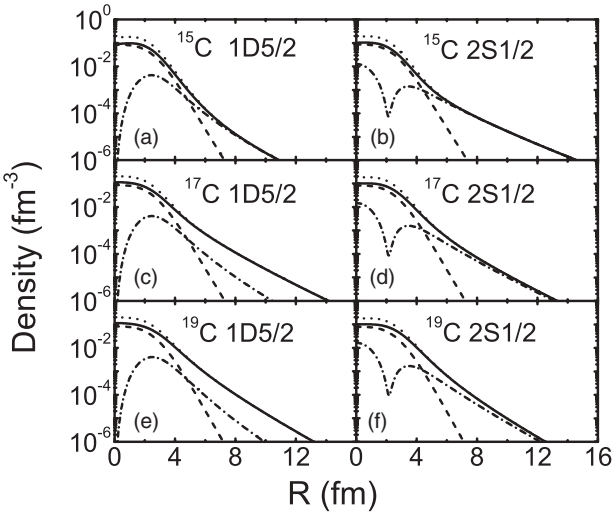

FIG. 4. Same as Fig. 2 but for ^{15,17,19}C.

^{19}C in case (a) are both larger than those in case (b). The reason is that in case (a) there are two neutrons in the $2s_{1/2}$ orbital, but in case (b) only one neutron occupies the $2s_{1/2}$ orbital. That is why the neutron radius of ^{17}C is the largest one in the C isotopes in the RMF theory. This agrees with the experimental fact [49]. This can be considered as an additional proof that the last neutron in ^{17}C occupies the $1d_{5/2}$ orbital rather than the $2s_{1/2}$ orbital. In Fig. 4 we show the density distributions of ^{15,17,19}C calculated from NL-SH. From this figure, one can see again that ^{15}C is a one-neutron halo nucleus when the last neutron occupies the $2s_{1/2}$ orbital, but the neutron densities of ^{17}C and ^{19}C are similar either the last neutron occupies the $1d_{5/2}$ orbital or occupies the $2s_{1/2}$ orbital. So it is impossible to determine the orbital of the last neutron only by comparing the neutron radii.

The form factors of these three nuclei when the last neutron occupies the same orbital are shown in Fig. 5. From this figure one can see that the form factors of these three nuclei are very close to each other. The difference is found only in higher q region ($q \geqslant 3.5$ fm $^{-1}$). In PWBA, the elastic magnetic form factor is the Fourier-Bessel transform of the current density which is directly related to the density distribution of the last nucleon. The form factor at large coordinate in momentum space is mainly determined by the current density at small coordinate in r space, and vice versa. The very close form factors in low and medium q region ($q \leqslant 3.5$ fm $^{-1}$) mean that the tail part of the wave functions of the last neutron in ^{15,17,19}C are very close to each other when the last neutron occupies the same orbital. When accurate experimental form factors in low and medium q region ($q \leqslant 3.5$ fm $^{-1}$) are obtained in the future, one can determine easily whether the last neutron of these nuclei occupies the same orbital by comparing the shape of the form factors.

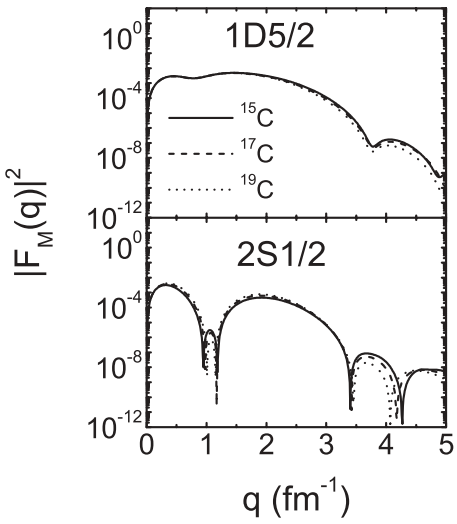

FIG. 5. Same as Fig. 3 but for ^{15,17,19}C.

At the same time one can see that there are great differences between the form factors for different configurations. When the form factors are measured, one can immediately determine the orbital of the last neutron by comparing the magnitude and shape of the experimental data with the theoretical curves. Furthermore one can deduce the wave function and density distribution of the last neutron.

According to above analyses, we conclude that the valence orbital of an odd-A exotic nucleus can be determined from the shape of the elastic magnetic form factor and then one can deduce the wave function and density distribution when the experimental data are available. What we are interested in is can we deduce the magnetic form factor when the valence density distribution are obtained from some method? The wave function and density distribution are determined by the node number, orbital angular momentum, and single-particle energy. In ^{15,17,19}C, the single-particle energies of the $1d_{5/2}$ and $2s_{1/2}$ orbitals are close, but the densities and rms radii differ greatly. It means that the density distribution of the last neutron is mainly dependent on the node number and the orbital angular momentum. Now we will investigate a pair of nuclei in which the last neutrons occupy the orbitals with the same node number and orbital angular momentum. ^{49}Ca and ^{59}Ca provide good examples. ^{49}Ca is another nucleus with a single neutron outside the doubly closed core. ^{59}Ca is found to be the odd-A neutron drip-line of Ca isotopes in the RMF theory [50]. The densities of the last neutron of ^{49}Ca and ^{59}Ca from NL-SH are shown in Fig. 6. From this figure one can see

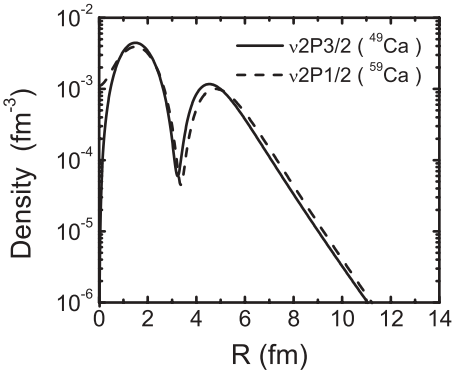

FIG. 6. The density distribution of the last neutron in ^{49}Ca and ^{59}Ca from NL-SH.

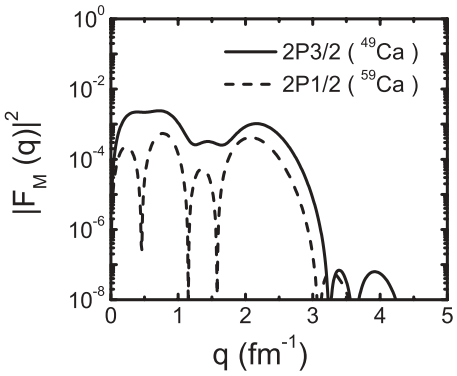

FIG. 7. Comparison of the calculated form factors of ^{49}Ca and ^{59}Ca from NL-SH.

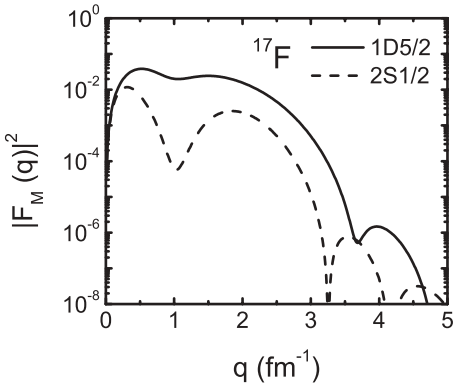

FIG. 8. Comparison of the calculated form factors of ^{17}F in the ground state and the first exited state.

that the shape of the densities are similar as expected, since the shape of the density is mainly determined by the node number and the orbital angular momentum (or centrifugal potential). The form factors of these two nuclei are shown in Fig. 7. It is clear that there are great differences between them. The magnitude of the form factor of ^{49}Ca is larger than that of ^{59}Ca. But the shapes of them are similar apart from the zero points which can be eliminated by considering the effect of Coulomb distortion. It means that the form factors are also dependent on the total angular momentum. The reason is that the magnetic form factor is determined by the magnetization density rather than the density distribution of the last nucleon.

Finally, we will investigate the magnetic form factors of proton halo nuclei. Due to the Coulomb barrier, proton halos may only occur at the proton drip-line of the lightest elements. Up to now, the only well-known example in ground state is ^{8}B. However, the RMF theory may be invalid for such a light nucleus. Another example is the first exited state of ^{17}F having the configuration $^{16}\mathrm{O}(0^+)\otimes 2s_{1/2}$ [51]. Its ground-state configuration is $^{16}\mathrm{O}(0^+)\otimes 1d_{5/2}$. Though it will be impossible to perform electron scattering experiments from the exited state of ^{17}F, it is also interesting to see whether the conclusions we have drawn from even-odd nuclei are applicable to odd-even ones where the convection currents exist. The form factors are shown in Fig. 8. It can be seen that the situation is similar to those of the even-odd nuclei ^{23}O and ^{15,17,19}C. So one can reach the same conclusion as those drawn from one-neutron halo nuclei.

IV. CONCLUSION AND DISCUSSIONS

In summary, the elastic magnetic electron scattering form factors of ^{23}O, ^{15,17,19}C, ^{49,59}Ca, and ^{17}F are calculated in the relativistic impulse approximation. Great differences between the form factors have been found when the last nucleon of a given nucleus occupies different orbitals. Therefore, one can determine immediately the orbital of the last nucleon when the form factors of these nuclei are measured. In this article the effects of various corrections such as backflow, MEC, and CP are neglected. Although great success has been achieved in treating the effects of backflow and MEC in the QHD framework, there are also many efforts should be made along this line. Ichii *et al*. [28] have examined the effect of backflow (vacuum fluctuation) in the Hartree approximation. Blunden *et al*. [30] have investigated the contribution of the one-pion exchange currents in the relativistic Hartree-Fock level. The effect of core polarization, which has been found to be important in the nonrelativistic theories [52,53], has not been treated consistently in the QHD framework. How to calculate these effects within the same model is an interesting problem. More detailed investigations are necessary in the future. Furthermore, the advent of the radioactive ion beam (RIB) gives us good chance to investigate some fundamental features about nuclear interaction. It is expected that the electron scattering from exotic nuclei will provide new information about the fundamental NN interaction. Our results will be useful for the electron scattering experiments in the near future.

ACKNOWLEDGMENTS

T.D. thanks Prof. Z. J. Wang for discussions on electron scattering. This work is supported by the National Natural Science Foundation of China (Grant Nos. 10535010, 10675090, 10775068), by the 973 National Major State Basic Research and Development of China (Grant No. 2007CB815000), by the CAS Knowledge Innovation Project No. KJCX2-SW-N02, and by the Research Fund of Education Ministry under Contract No. 20010284036.

[1] I. Tanihata, J. Phys. G **22**, 157 (1996).
[2] I. Tanihata, in *Nuclei at Extremes of Isospin and Mass*, edited by A. Ansari and R. K. Choudhury (Narosa, New Delhi, 2005), p. 1.
[3] B. Jonson, Phys. Rep. **389**, 1 (2004).
[4] Z. Wang and Z. Ren, Phys. Rev. C **70**, 034303 (2004); **71**, 054323 (2005); Zaijun Wang, Zhongzhou Ren, and Ying Fan, *ibid*. **73**, 014610 (2006).

[5] R. Kanungo, M. Chiba, N. Iwasa, S. Nishimura, A. Ozawa, C. Samanta, T. Suda, T. Suzuki, T. Yamaguchi, T. Zheng, and I. Tanihata, Phys. Rev. Lett. **88**, 142502 (2002).
[6] B. A. Brown, P. G. Hansen, and J. A. Tostevin, Phys. Rev. Lett. **90**, 159201 (2003).
[7] R. Kanungo, M. Chiba, N. Iwasa, S. Nishimura, A. Ozawa, C. Samanta, T. Suda, T. Suzuki, T. Yamaguchi, T. Zheng, and I. Tanihata, Phys. Rev. Lett. **90**, 159202 (2003).
[8] D. Cortina-Gil *et al*., Phys. Rev. Lett. **93**, 062501 (2004).
[9] C. Nociforo *et al*., Phys. Lett. **B605**, 79 (2005).
[10] Z. Elekes *et al*., Phys. Rev. Lett. **98**, 102502 (2007).
[11] D. Bazin *et al*., Phys. Rev. Lett. **74**, 3569 (1995); D. Bazin *et al*., Phys. Rev. C **57**, 2156 (1998).
[12] T. de Forest and J. D. Walecka, Adv. Phys. **15**, 1 (1966).
[13] T. W. Donnelly and J. D. Walecka, Nucl. Phys. **A201**, 81 (1973).
[14] T. W. Donnelly and I. Sick, Rev. Mod. Phys. **56**, 461 (1984).
[15] T. Suda, K. Maruyama, and I. Tanihata, RIKEN Accel. Prog. Rep. **34**, 49 (2001).
[16] T. Suda and M. Wakasugi, Prog. Part. Nucl. Phys. **55**, 417 (2005).
[17] G. Münzenberg, in *Nuclei at Extremes of Isospin and Mass*, edited by A. Ansari and R. K. Choudhury (Narosa, New Delhi, 2005), p. 18.
[18] An international accelerator facility for beams of ions and antiprotons, GSI report, 2002.
[19] C. A. Bertulani, Phys. Lett. **B624**, 203 (2005).
[20] S. Karataglidis and K. Amos, Phys. Lett. **B650**, 148 (2007).
[21] G. Audi and A. H. Wapstra, Nucl. Phys. **A595**, 409 (1995).
[22] G. Audi, A. H. Wapstra, and C. Thibault, Nucl. Phys. **A729**, 337 (2003).
[23] T. Nakamura, N. Fukuda, T. Kobayashi, N. Aoi, H. Iwasaki, T. Kubo, A. Mengoni, M. Notani, H. Otsu, H. Sakurai, S. Shimoura, T. Teranishi, Y. X. Watanabe, K. Yoneda, and M. Ishihara, Phys. Rev. Lett. **83**, 1112 (1999).
[24] Z. Ren, W. Mittig, B. Chen, and Z. Ma, Phys. Rev. C **52**, R20 (1995); Z. Ren, W. Mittig, B. Chen, Z. Ma, G. Auger, and G. Xu, *ibid*. **52**, R1764 (1995); Z. Ren, B. Chen, Z. Ma, and G. Xu, *ibid*. **53**, R572 (1996).
[25] B. D. Serot, Phys. Lett. **B107**, 263 (1981).
[26] E. J. Kim, Phys. Lett. **B174**, 233 (1986).
[27] T. Matsui, Nucl. Phys. **A370**, 365 (1981).
[28] S. Ichii, W. Bentz, A. Arima, and T. Suzuki, Nucl. Phys. **A487**, 493 (1988).
[29] R. J. Furnstahl and C. E. Price, Phys. Rev. C **40**, 1398 (1989).
[30] P. G. Blunden and E. J. Kim, Nucl. Phys. **A531**, 461 (1991).
[31] G. A. Lalazissis, J. König, and P. Ring, Phys. Rev. C **55**, 540 (1997).
[32] M. M. Sharma, M. A. Nagarajan, and P. Ring, Phys. Lett. **B312**, 377 (1993).
[33] Y. Sugahara and H. Toki, Nucl. Phys. **A579**, 557 (1994).
[34] J. D. Bjorken and S. D. Drell, *Relativistic Quantum Mechanics* (McGraw-Hill, New York, 1964).
[35] B. D. Serot and J. D. Walecka, in *The Relativistic Nuclear Many-Body Problem*, Advances in Nuclear Physics, Vol. 16, edited by J. W. Negele and E. Vogt (Plenum Press, New York, 1986).
[36] J. D. Walecka, *Electron Scattering for Nuclear and Nucleon Structure* (Cambridge University Press, Cambridge, 2001).
[37] A. R. Edmonds, *Angular Momentum in Quantum Mechanics* (Princeton University Press, Princeton, New Jersey, 1960).
[38] R. S. Willey, Nucl. Phys. **40**, 529 (1963).
[39] P. Raghavan, At. Data Nucl. Data Tables **42**, 189 (1989).
[40] N. Kalantar-Nayestanaki *et al*., Phys. Rev. Lett. **60**, 1707 (1988).
[41] S. Burzynski, M. Baumgartner, H. P. Gubler, J. Jourdan, H. O. Meyer, G. R. Plattner, H. W. Roser, and I. Sick, Nucl. Phys. **A399**, 230 (1983).
[42] R. S. Hicks, Phys. Rev. C **25**, 695 (1982).
[43] M. V. Hynes *et al*., Phys. Rev. Lett. **42**, 1444 (1979).
[44] G. D. Jones, J. L. Durell, J. S. Lilley, and W. R. Phillips, Nucl. Phys. **A230**, 173 (1974).
[45] J. L. Durell, C. A. Harter, J. N. Mo, and W. R. Phillips, Nucl. Phys. **A334**, 144 (1980).
[46] S. Platchkov *et al*., Phys. Rev. Lett. **61**, 1465 (1988).
[47] H. Baghaei *et al*., Phys. Rev. C **42**, 2358 (1990).
[48] J. Dechargé and D. Gogny, Phys. Rev. C **21**, 1568 (1980).
[49] E. Liatard *et al*., Europhys. Lett. **13**, 401 (1990).
[50] M. Bhattacharya and G. Gangopadhyay, Phys. Rev. C **72**, 044318 (2005).
[51] R. Morlock, R. Kunz, A. Mayer, M. Jaeger, A. Müller, J. W. Hammer, P. Mohr, H. Oberhummer, G. Staudt, and V. Kölle, Phys. Rev. Lett. **79**, 3837 (1997).
[52] I. S. Towner, Phys. Rep. **155**, 263 (1987).
[53] P. G. Blunden and B. Castel, Nucl. Phys. **A445**, 742 (1985).